Clim Dyn (2015) 44:2683–2702
DOI 10.1007/s00382-014-2425-9

A case study of the impact of boreal summer intraseasonal oscillations on Yangtze rainfall

Jianying Li · Jiangyu Mao · Guoxiong Wu

Received: 11 January 2014 / Accepted: 19 November 2014 / Published online: 2 December 2014

Abstract The impact on Yangtze rainfall of the boreal summer intraseasonal oscillations (BSISOs) over the entire Asian summer monsoon region during summer 1996 was investigated using the APHRODITE gridded rainfall and the NCEP–DOE reanalysis II products. Wavelet analyses suggest that the ISOs of Yangtze rainfall were regulated mainly by both 30–60- and 10–25-day oscillations, respectively linked to BSISO1 and BSISO2 activity. Phase locking of the wet phases of these two ISOs resulted in a prolonged wet episode from late June to mid-July. The circulation evolution of the BSISO1 mode showed that active convection accompanied by strong convergence of anomalous zonal winds first developed over the equatorial Indian Ocean, with suppressed convection over the South China Sea (SCS)–Philippine Sea and with active convection over the Yangtze Basin. The triple convection anomaly that aligned meridionally in the East Asian sector arose from a local meridional–vertical cell associated with a Rossby wave-like coupled circulation–convection system. The opposite flow patterns occurred during the dry phase of Yangtze rainfall. The composite BSISO2 cases demonstrated a weak convective anomaly initially appeared around the Maritime Continent, with a huge anomalous anticyclone accompanied by suppressed convection over the SCS–Philippine Sea. The low-level convergence of the anomalous southwesterlies on the northwestern side of the anticyclone and the consequent ascent led to positive rainfall anomalies over the Yangtze Basin. When the entire SCS was dominated by an anomalous cyclone resulting from interaction with upstream systems, convection over the Yangtze Basin was suppressed.

Keywords Boreal summer intraseasonal oscillations · Yangtze rainfall · Prolonged wet episode · Coupled circulation–convection system

J. Li · J. Mao (✉) · G. Wu
State Key Laboratory of Numerical Modeling for Atmospheric Sciences and Geophysical Fluid Dynamics (LASG), Institute of Atmospheric Physics, Chinese Academy of Sciences, P.O. Box 9804, Beijing 100029, China
e-mail: mjy@lasg.iap.ac.cn

J. Li
University of Chinese Academy of Sciences, Beijing 100049, China

1 Introduction

The East Asian summer monsoon (EASM) is one of the important components of the Asian summer monsoon (ASM), covering a large area from tropical Southeast Asia to extratropical Northeast Asia (Lau et al. 1988). The dominant circulation system in the EASM that affects the weather and climate over extratropical regions is the Meiyu (in eastern China)–Baiu (in Japan)–Changma (in Korea) front, one of the major convergence zones of the global atmospheric circulation (Chen et al. 2000). In eastern China, heavy rainfall usually occurs over the Yangtze Basin with the establishment of the Meiyu front around mid-June, due to the northward seasonal March of the EASM. However, the intraseasonal spatio-temporal evolution of the EASM circulation system exhibits substantial year-to-year variability. The timing of the onset of the EASM and the timing of the active and break periods of the Meiyu front vary from year to year. As pointed out by Webster et al. (1998), a late or early onset of the monsoon or an ill-timed lull in the monsoon rains may have devastating effects on agriculture even if the annual mean rainfall is normal. Furthermore, the intraseasonal anomalies associated with variations in the

large-scale monsoon circulation may be crucial in determining the seasonal-mean rainfall. For example, the 1991 flood over the Yangtze Basin in summertime was associated with a strong 15–35-day oscillation (Mao and Wu 2006), and the 1998 flood over eastern China was related to the 30–60-day oscillation over the western North Pacific (WNP; Zhu et al. 2003). Although these intraseasonal oscillations (ISOs) of Yangtze rainfall may be linked with tropical intraseasonal systems over the equatorial WNP that propagate northward and/or northwestward, as was suggested by Mao et al. (2010), where do the equatorial WNP intraseasonal systems originate? Note that tropical intraseasonal variability has been suggested as a key source of untapped predictability for the extended-range forecasts in both the tropics and extratropics (e.g., Waliser et al. 2003). Thus, studying the physical relationship between the ISOs of Yangtze rainfall and tropical intraseasonal variability is important for improving predictive skill on intraseasonal and seasonal timescales based on dynamical or statistical models.

The intraseasonal variability, an important component of monsoon variability within the annual cycle, is a fundamental feature of the ASM. Over the South Asian monsoon region, the intraseasonal fluctuations of the monsoonal rainfall in most summers are dominated by the 30–60-day (interchangeably the 30–40-day) oscillation (e.g., Krishnamurti and Subrahmanyam 1982; Murakami and Nakazawa 1984; Lau and Chan 1986; Lau and Peng 1987), and this 30–60-day oscillation exhibits distinct northward movement while propagating to the east (e.g., Lawrence and Webster 2002; Jones et al. 2004). There is another pronounced 10–25-day (interchangeably the 10–20- or 10–30-day) oscillation that migrates westward and northwestward over the vast EASM region (e.g., Chen and Chen 1995; Mao and Chan 2005; Zhou and Chan 2005). These ISOs from the tropics modulate the ASM activity, with episodes of abundant rainfall (active phases) separated by dry spells (break phases), which cause floods and droughts over parts of the ASM region, such as the Yangtze flood in 1996 and the Indian continental drought in 2002. The 1996 Yangtze flood with seasonal (May–October) rainfall excess above 40 % may have resulted from an unusually prolonged episode of active monsoon from late June to mid-July, while the 2002 Indian drought was primarily due to an unprecedented break in the summer monsoon during July, with a seasonal (June–September) all-Indian rainfall deficit of 21.5 % (Bhat 2006). Obviously, the behavior and impact of tropical ISOs on the ASM over different areas vary from year to year. The interannual variability of the ISOs affecting the ASM in terms of strength and propagating characters has been suggested to be related to external forcing such as sea surface temperature (SST) anomalies in the Pacific and Indian Oceans (e.g., Lawrence and Webster 2001). Ajayamohan et al. (2008) noticed that the poleward propagation of boreal summer ISOs (BSISOs) is evidently influenced by the Indian Ocean Dipole (IOD; Saji et al. 1999), with coherent (incoherent) poleward propagation of precipitation anomalies from 5°S to 25°N over the South Asian Monsoon sector during negative (positive) IOD years, although Lawrence and Webster (2001) suggested the BSISO activities being not highly dependent on the state of El Niño–Southern Oscillation (ENSO). Whereas such interannual variations of the BSISO activities influencing the EASM with association with IOD or ENSO are not clear, thus the typical case study of BSISO activities in relation to the EASM strength under an IOD or ENSO background is conducive to understanding the BSISO activity–EASM relationship. For example, the 1996 summer just belonged to a negative IOD year, how and to what extent did the BSISO activities result in the 1996 Yangtze flood during this summer? The physical processes and implication of such a BSISO activity–EASM relationship deserve further investigation.

Many previous studies have examined ISO behaviors over different parts of Asia (e.g., Mao and Wu 2006; Guan and Chan 2006; Hoyos and Webster 2007; Yang et al. 2009). Bandpass-filtering is often used to extract the frequency-limited signal; however, this requires information beyond the end of the time series, and is not useful for real-time monitoring and forecasting. Wheeler and Hendon (2004) proposed an all-season Real-time Multivariate MJO (RMM) index (RMM1 and RMM2), based on the fundamental characteristics of the Madden–Julian oscillation (MJO; Madden and Julian 1971, 1972), a planetary-scale eastward-propagating wave-like mode with coherent fluctuations in convection and winds. Such an index could be used to monitor prominent MJO events in tropics and to identify the MJO's impact on Australian rainfall (Wheeler et al. 2009). The MJO is most active in the boreal winter, while its counterpart (usually the ISO) in the boreal summer exhibits distinct poleward-propagating characteristics, as reported by Jones et al. (2004). Although the RMM index captures well the eastward-propagating characteristic of the MJO along the equator, it fails to represent the behavior of the BSISO involving both distinct eastward- and northward-propagation in the ASM regime. Lee et al. (2013) therefore recently suggested two real-time BSISO indices (BSISO1 and BSISO2) obtained from Multivariate Empirical Orthogonal Function (MV-EOF) analysis of outgoing long-wave radiation (OLR) and zonal wind at 850 hPa. BSISO1 is defined by the first two principal components (PCs) of the MV-EOF analysis, which together represent the canonical northward propagating variability with quasi-oscillatory periods of 30–60 days that often occurs in conjunction with the eastward MJO. BSISO2 is defined by the third and fourth PCs, which together mainly capture the northward or northwestward propagating variability with periods of 10–30 days that occurs primarily during the pre-monsoon and monsoon-onset seasons.

As suggested by Lee et al. (2013), BSISO1 better represents the northward-propagating pattern over the ASM region than does the RMM (Wheeler and Hendon 2004). The evolution (see composites in Fig. 9 of Lee et al. 2013) of the BSISO1 circulation pattern, with a northwest to southeast slope, demonstrates that anomalous convection occurs firstly over the equatorial Indian Ocean (EIO) in phase 1. It then propagates northward, reaching the Indian Subcontinent in phase 3 and the Bay of Bengal in phases 4–5, reproducing well the northward movement over the South Asian sector that is directly related to the eastward propagation of the ISO (Lawrence and Webster 2002). The anomalous convection over the EIO also propagates eastward into the Maritime Continent in phases 3–4, and subsequently propagates northward in phases 5–8, reaching the South China Sea (SCS) in phase 7, and the WNP in phase 8. Relatively weak convection anomalies exist over the extratropical East Asian area, especially over the Yangtze Basin during phases 3–4 and phases 7–8, resulting from anomalous southwesterlies (northeasterlies) on the northwestern side of the anticyclone (cyclone) over the SCS–WNP. These variations in circulation over the EASM sector illustrate more clearly the close link between the ISO that propagates northward from the equatorial western Pacific to the northern SCS and the signal propagating eastward from the EIO. They also demonstrate that the ISOs of Yangtze summer rainfall are directly associated with a northward-propagating Rossby wave-like coupled circulation–convection system (Mao et al. 2010), indicating that the intraseasonal behavior of the Yangtze rainfall may be monitored using the BSISO1 index.

The BSISO2 circulation structure is more elongated and front-like with a southwest to northeast slope (Lee et al. 2013). The series of composites shows that anomalous convection locates in the EIO and Philippine Sea in phase 1, which then propagates northwestward over the Indian longitudes and the WNP–East Asia region. Note that the convection anomalies over central southern China and the SCS–WNP are out of phase in phases 3–4 and 6–7; this bears some resemblance to the seesaw pattern in rainfall anomalies between the Yangtze Basin and the SCS–Philippine Sea (Mao et al. 2010). Thus, the intraseasonal rainfall variability over the Yangtze Basin and southern China is likely related to BSISO2.

One of the objectives of the present study is therefore to examine how the ISOs of Yangtze rainfall relate to the BSISO behaviors over the entire ASM region, based on a case study of the summer of 1996, and thus to understand the mechanism responsible for the severe Yangtze floods in terms of intraseasonal variability. There are at least three reasons why the 1996 summer is selected as a representative case for present study. Firstly, although the intraseasonal variability of Yangtze rainfall in amplitude and frequency varies from year to year, for most of Yangtze flooding years the rainfall evolutions in intensity usually exhibit pronounced ISOs during summer season (Huang et al. 2008), with a series of heavy rain events occurring over the Yangtze Basin, indicating that the ISOs are the dominant source of short-term climate variability over the Yangtze Basin. Again, we examined the interannual variations of Yangtze summer-mean rainfall and intraseasonal anomaly rainfall, and found most of the flooding years being accompanied by strong ISOs. Though maximum rainfall anomalies associated with larger intraseasonal standard deviations may not always appear over the exact same locations within Yangtze Basin among flooding years, they mostly occur around the middle and lower Yangtze Basin. The Yangtze flood in the 1996 summer was one of such severe floods occurring over the middle and lower Yangtze Basin, being a typical flooding case associated with the EASM activities. Secondly, during the 1996 summer active and break sequences of Yangtze rainfall was dominated by both 30–60- and 10–25-day ISOs (as discussed below), with such two ISOs respectively matching the frequencies of BSISO1 and BSISO2 modes (Lee et al. 2013), indicating a close connection of intraseasonal Yangtze rainfall with tropical signal sources. Thirdly, as suggested by Ajayamohan et al. (2008), the IOD may exert an influence on BSISO activities, with the 1996 summer being a negative IOD year, thus the case study for the 1996 summer facilitates to demonstrate the association of BSISO activities with intraseasonal Yangtze rainfall and possible impacts of the IOD on such an association over the East Asia–Western Pacific sector.

Although seamless seasonal prediction will eventually rely on numerical dynamic models, current state-of-the-art climate models still have difficulties in simulating and forecasting intraseasonal variability (Huang et al. 2013), while statistical approaches exhibit some skill in forecasting ISOs (e.g., Hoyos and Webster 2007). Therefore, another objective of this paper is to investigate the potential application of the BSISO indices to retrieving the intraseasonal variability of the subtropical summer monsoon, forming a possible scenario to predict the intraseasonal Yangtze rainfall anomalies by constructing a statistical model with BSISO indices.

The remainder of this paper is organized as follows. Section 2 describes the data and methods, while the intraseasonal variation of Yangtze rainfall during the extended summer (May–October) of 1996 is outlined in Sect. 3. Section 4 examines the spatio-temporal evolution of the BSISO modes and their impact on Yangtze rainfall. Section 5 presents an application of BSISO indices to retrieving the intraseasonal Yangtze rainfall anomalies. Finally, a summary and discussion are given in Sect. 6.

2 Data and methods

2.1 Data

Daily gridded rainfall data with a horizontal resolution of 0.25° × 0.25° are obtained from the Asian Precipitation-Highly Resolved Observational Data Integration Towards the Evaluation of Water Resources (APHRODITE) project (Yatagai et al. 2009), which uses primarily rain-gauge observations across Asia (Yatagai et al. 2012). Currently, these high-resolution precipitation products are only available from 1951 to 2007, with the daily long-term mean calculated for the period 1981–2007. Daily atmospheric circulation data including three-dimensional wind components and relative humidity are extracted from the National Centers for Environmental Prediction–Department of Energy (NCEP–DOE) Atmospheric Model Inter-comparison Project (AMIP-II) reanalysis (Kanamitsu et al. 2002). Daily OLR data from the National Oceanic and Atmospheric Administration (NOAA) polar-orbiting satellites are used as a proxy for tropical deep convection (Liebmann and Smith 1996). Both OLR and NCEP–DOE reanalysis II data have a horizontal resolution of 2.5° longitude × 2.5° latitude, and cover the period 1981–2010.

2.2 Methods

The BSISO indices during the 1996 summer (actually during each of all summers) were derived from the exact same MV-EOF analysis of daily mean OLR and 850-hPa zonal wind anomalies as in Lee et al. (2013) over the entire ASM region (10°S–40°N, 40°–160°E) for the extended boreal summer (May–October) season over the 30-year period 1981–2010, in which intraseasonal OLR and 850-hPa zonal wind anomalies at each grid point were calculated by removing the slow annual variation (mean and first three harmonics of climatological annual cycle) and the effect of interannual variability (by subtracting a 120-day running mean of the last 120 days). Likewise, such time filtering was applied to other variables such as rainfall and vertical motion in order to produce the intraseasonal anomaly time series. Considering the present case study, some high-frequency synoptic fluctuations had to be removed after finishing all the above calculations. Thus a 10-day running mean was applied to the intraseasonal anomaly time series of each variable during the 1996 summer. To explore the respective impacts of BSISO1 and BSISO2 on the Yangtze rainfall during the 1996 summer, BSISO1- and BSISO2-related intraseasonal rainfall anomalies were estimated from multiple linear regression of precipitation against the BSISO1 and BSISO2 indices, respectively. Additionally, composite analyses of intraseasonal anomalies of the related variables were performed to better understand the regression results in terms of dynamical processes. Several associated variables (e.g., vertical velocity, OLR, 850- and 200-hPa winds) were used to examine the spatio-temporal structure of the intraseasonal Yangtze rainfall in relation to the activity of the BSISO1 or BSISO2. The statistical significance of the composite anomalies was estimated based on Student's t test, in which the effective sample size of the intraseasonal anomaly time series for a particular variable was calculated using the method of Bretherton et al. (1999), since the above time filtering could reduce the degree of freedom of intraseasonal anomaly time series.

As a powerful technique for time–frequency decomposition of a time series, wavelet analysis was applied to the time series of the Yangtze rainfall anomaly to identify the dominant ISO periods, choosing the sixth-order derivative of a Gaussian function as the wavelet basis function to better resolve the abrupt temporal variations in Yangtze rainfall (e.g., Torrence and Compo 1998).

3 Anomalous Yangtze rainfall during the 1996 summer

Since summertime rainfall amount is one of the most important indicators of the EASM, the distribution of percentage of the 1996 summer total rainfall anomalies relative to the long-term mean period 1981–2007 are shown in Fig. 1, together with the distribution of the standard deviation of the daily intraseasonal rainfall anomaly. Maximum positive anomalies (>40 %) were observed over the Yangtze Basin, accompanied by large standard deviations of intraseasonal rainfall variability in excess of 6 mm day^{-1}, indicating that Yangtze rainfall in this year was controlled by strong ISOs. Note that the negative anomalies south of the Yangtze Basin corresponded to relatively weak intraseasonal variations.

A similar situation occurred during the traditional summer season from June to August (JJA) (not shown). Both the percentage of the JJA-mean rainfall anomalies and the amplitude of the ISOs were comparable to those in Fig. 1, indicating that the 1996 Yangtze flood was dependent largely on the JJA anomalous rainfall.

The time series of the area-averaged Yangtze rainfall anomalies in Fig. 2a highlighted the considerable differences between the 1996 Yangtze rainfall and the climatological situation on the intraseasonal timescale. There was a short period with positive rainfall anomalies at the beginning of May followed by negative anomalies in most of May, and then a distinct wet phase was observed in early June, followed by one and a half weeks of dry conditions in mid-June. The period from late June to middle July was predominately wet, with mostly weaker rainfall from then until the end of October. The long wet episode from late June to mid-July resulted in the flooding over the Yangtze Basin. Similar intraseasonal variations and resultant flooding have also been found in other summers (e.g., Mao and Wu 2006).

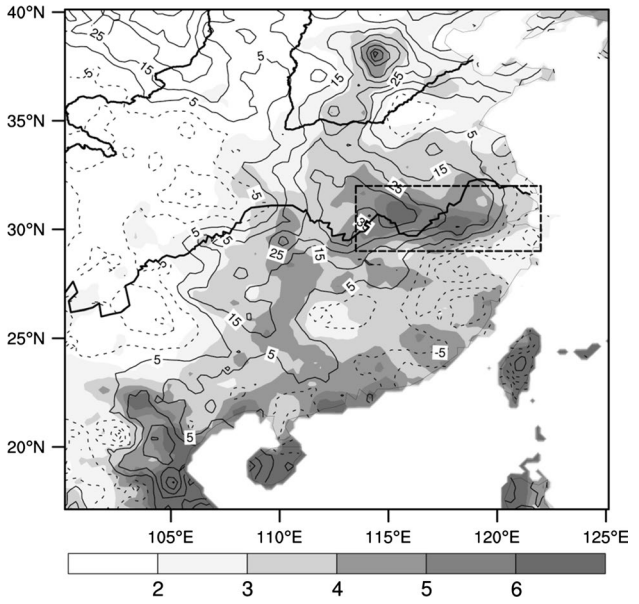

Fig. 1 Distributions of percentage of the 1996 summer (1 May to 31 October) rainfall anomalies from the 1981–2007 climatology (*contours*, %) and intraseasonal standard deviations (*shading*, mm day^{-1}) for the 1996 summer. The contour interval is 10 %, with *dashed contours* denoting negative rainfall anomalies. The *rectangular area* denotes the Yangtze Basin (29°–32°N, 113.5°–122°E) over which the area-averaged rainfall time series is produced in Fig. 2

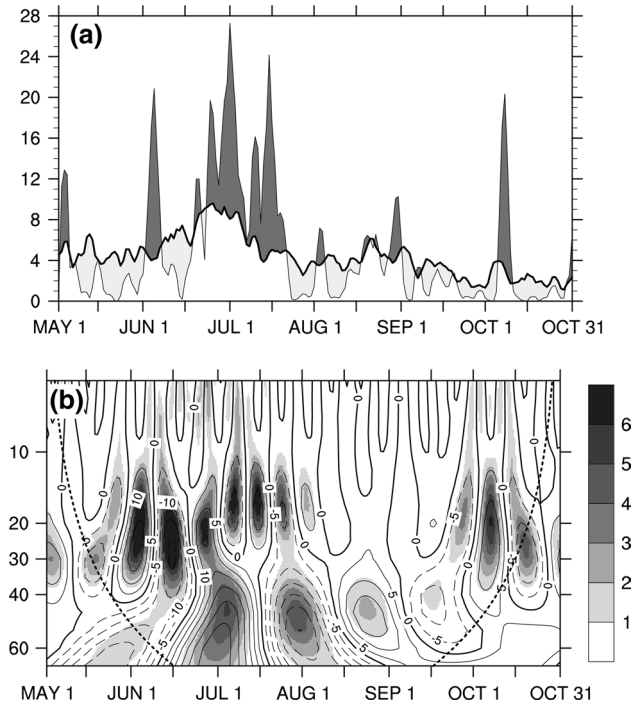

Fig. 2 **a** Time series of the 3-day running mean rainfall (*thin curves*, mm day^{-1}) for the period 1 May to 31 October 1996, area-averaged over the Yangtze Basin (29°–32°N, 113.5°–122°E). Also shown is the area-averaged climatological summer rainfall (*thick curves*, mm day^{-1}) calculated from daily rainfall data from 1981 to 2007. *Positive* (*negative*) rainfall anomalies with respect to the climatology are *darkly* (*lightly*) *shaded*. **b** Wavelet power spectra (*contours*) of the time series of the area-averaged Yangtze intraseasonal rainfall anomalies for the 1996 summer (1 May to 31 October) shown in (**a**) using the sixth-order derivative of a Gaussian as wavelet basis function. The *contour* interval for the spectrum coefficients is 5, with the zero contour *thickened* and negative contours *dashed*. The *shading* indicates regions of >95 % confidence level for a red-noise process. The *thick dashed line* denotes the cone of influence outside which the edge effects become important

The wavelet spectra demonstrate that the ISOs of Yangtze rainfall in summer 1996 were controlled by two dominant ISO modes, one with period in the range 30–60 days and the other in the range 10–25 days (Fig. 2b). The prolonged wet episode from late June to mid-July in Fig. 2a appears to result from a phase-lock between a wet phase of the 30–60-day ISO and two wet phases of the 10–25-day ISO. Note also that the intervening dry phase of the 10–25-day ISO counteracted some of the strong precipitation during the wet phase of the 30–60-day ISO, leading to a short period of reduced rainfall within this long wet episode. The magnitude of the wavelet power spectra denotes the strength of the ISO. While both of these two frequency bands passed the 95 % significance test for red noise, the 30–60-day oscillation was much stronger than the 10–25-day oscillation, consistent with the result of Huang et al. (2008).

The frequencies of these two dominant oscillations of Yangtze rainfall agreed well with the BSISOs (Lee et al. 2013). To demonstrate the association of intraseasonal Yangtze rainfall with BSISOs, the distributions of variances explained by BSISO1- and BSISO2-related rainfall anomalies over eastern China are shown in Fig. 3. The explained variance for each grid cell was calculated as the square of the correlation coefficient between the time series of the actual rainfall anomalies and the BSISO1-related (BSISO2-related) rainfall anomalies. The area of significantly large variances explained by BSISO1-related rainfall anomalies is mainly confined to the Yangtze Basin (Fig. 3a), while the significant variances explained by BSISO2 covered both the Yangtze Basin and southern China (Fig. 3b), indicating that the ISOs of Yangtze rainfall were indeed linked with the intraseasonal behavior of the entire ASM. Note again that the influence of the BSISO1 mode (26 %) was much greater than that of BSISO2 (13.7 %) over the Yangtze Basin.

4 Impact of the BSISO modes on Yangtze rainfall anomalies

4.1 Impact of BSISO1

As analyzed above, the prolonged wet episode over the Yangtze Basin from late June to mid-July arose from the

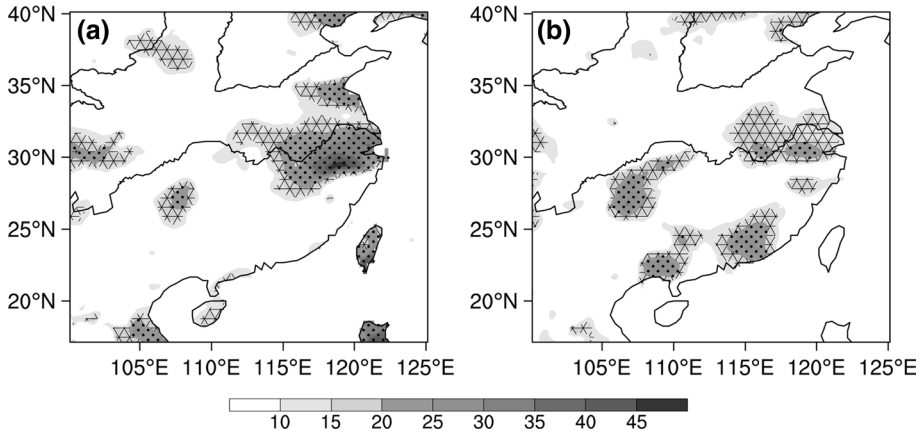

Fig. 3 Distributions of intraseasonal rainfall variances (*shading*, %) explained by **a** BSISO1-related and **b** BSISO2-related rainfall anomalies for the period 1 May to 31 October 1996. The cross-hatching (*dot-hatching*) indicates the regions where the variances are statistically significant at the 90 % (95 %) confidence level

superposition of the wet phases of the local 30–60-day oscillation and the local 10–25-day oscillation, with the former associated with the BSISO1 mode and the latter related to the BSISO2 mode. As shown in Fig. 2, this prolonged wet episode corresponded to the active phase of the strongest 30–60-day oscillation locally in the Yangtze Basin, which lasted from 26 June to 14 August. Thus, this case was selected to illustrate the impact of the BSISO1 on Yangtze rainfall. The phase-space representation of the BSISO1 index during the selected period is shown in Fig. 4. Each point in this two-dimensional phase space defined by the standardized PC1 and PC2 represents the state of BSISO1 at a particular time.

This strong BSISO1 case can be identified in phase-space, in which the amplitude $[(PC1^2 + PC2^2)^{1/2}]$ of the BSISO1 index exceeds the amplitude threshold of 1.0 on most days. The position of each point also represents the geographical location where deep convection occurred. Deep convection initially arose over the EIO at several points in late June, mostly concentrated in phase 1 and phase 2. Deep convection subsequently strengthened locally, stagnated for more than 2 weeks, and then quickly migrated northeastward into the southern SCS on 16 July. Note that this period coincided with the Yangtze wet episode. Afterwards, deep convection continually migrated northward in the SCS till the end of July, where it remained for more than 10 days. From the beginning of August, deep convection over the SCS gradually decayed and retreated eastward, indicating the end of the BSISO1 event.

To further demonstrate how BSISO1 mode influences Yangtze rainfall, Fig. 5 presents the evolution of this strong BSISO1 case in terms of 6-day mean OLR and 850-hPa wind anomalies. Active convection anomalies were observed to occur over the EIO from 26 June to 1 July, accompanied by strong convergence of anomalous zonal winds. The equatorial westerly anomalies resulted from the cyclone pair on either side of the equator, while the

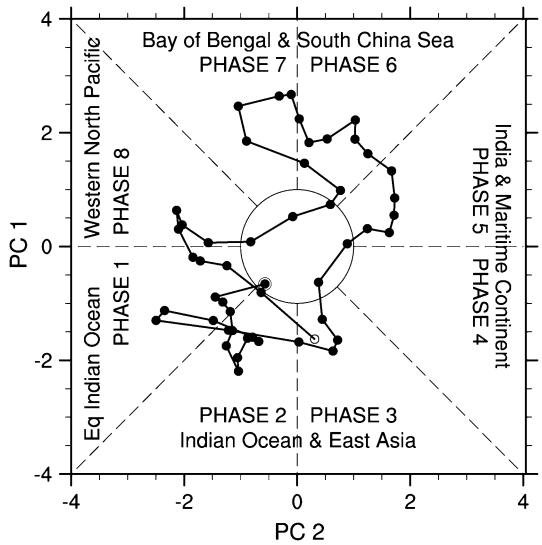

Fig. 4 Phase-space representation of the two-principal-component (PC) BSISO1 index (PC1 and PC2) for the period 26 June to 14 August 1996, with each dot representing the amplitude of the index on a particular day. Also shown are the eight defined phases of the BSISO1 and the region (*central circle*) where the BSISO1 index amplitude $(PC1^2 + PC2^2)^{1/2}$ is <1.0, corresponding to weak activity. The approximate locations of the propagating active convective signal of the BSISO1 are also shown for each quadrant of phase space. *Solid* (*open*) *circle* indicates the *starting* (*end*) point

equatorial easterly anomalies over the Maritime Continent came from the anomalous anticyclone associated with significantly suppressed convection over the SCS–Philippine Sea. On the northwestern side of the anomalous anticyclone, anomalous southwesterlies converged toward the Yangtze Basin, producing active convection. This might suggest that rainfall anomalies over the Yangtze Basin occur in conjunction with those over the EIO and SCS–Philippine Sea regions on intraseasonal timescales. The entire flow pattern in this phase exhibited similar features to the typical BSISO1 composite structure (see phase 1 in fig. 9 of Lee et al. 2013).

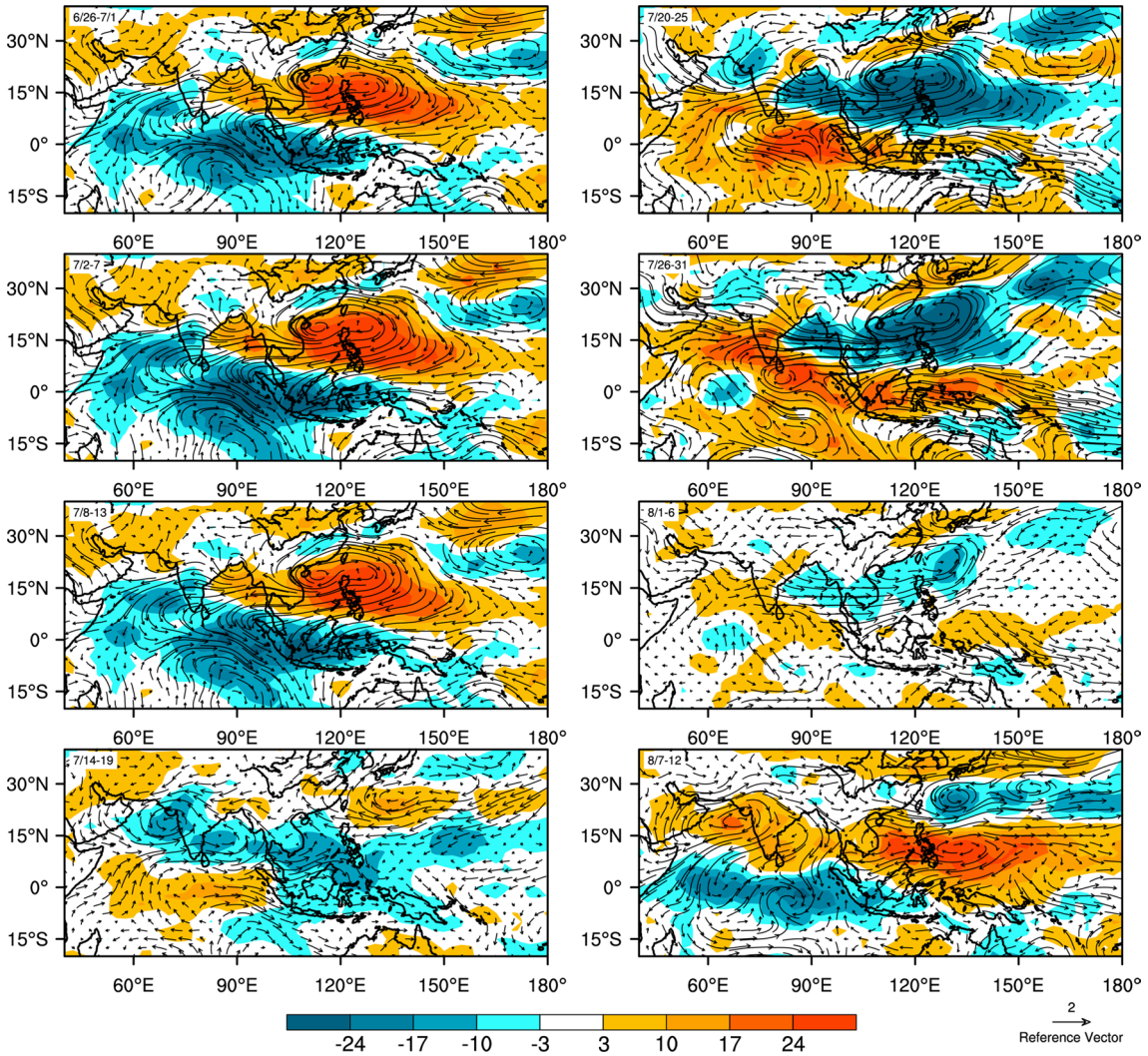

Fig. 5 Evolution of 6-day mean OLR (*color scale*, W m^{-2}) and 850-hPa wind (*vectors*, m s^{-1}) anomalies for the BSISO1 case from 26 June to 12 August 1996. The magnitude of the reference *vector* is provided at *bottom right*

Subsequently, the active convection strengthened over the western Maritime Continent, but the overall circulation structure remained almost unchanged until 13 July, indicating that during the first three 6-day the evolutions of this BSISO1 case differed from the those of typical BSISO1 event in phases 1–3 (see Lee et al. 2013) in terms of slower propagation or even stagnation. Note that convective anomalies both north and south of the SCS were opposite in sign to those over the SCS, forming a triple convection anomaly pattern along the meridian from the Maritime Continent to the Yangtze Basin. Such a triple rainfall anomaly might be caused by a local meridional–vertical cell, associated with the northward movement of a Rossby wave-like coupled circulation–convection system along the East Asian coast (as discussed below). Note that the basic flow structure, together with the deep convection over the EIO prior to 13 July, could be characterized as a convectively coupled Kelvin–Rossby wave packet (Wang and Rui 1990; Zhang 2005) and is similar to the analytical solution of heat-induced tropical circulation for symmetric heating about the equator (Gill 1980), suggesting that convective feedback with wave dynamics played an important role in the formation and development of the BSISO1 event. As to why active convection anomalies kept almost stagnant over the EIO for more than 2 weeks, this question will be discussed in Sect. 4.3.

The active convection continued to migrate northward, as for a typical BSISO1 event. By 14–19 July, the active convection reached the SCS in conjunction with an anomalous elongated off-equator cyclone cluster extending from the northern Arabian Sea to the SCS, which resulted from the EIO cyclonic anomaly migrating northward into the Northern Hemisphere. The anomalous anticyclone over the SCS–Philippine Sea thus weakened significantly

and moved northeastward out of the SCS to around 30°N in such a way that the Yangtze Basin was dominated by the lower-level divergent conditions. Convective activities over the EIO were suppressed, forming a west–east oriented dipole-heating anomaly with the active convection over the SCS. In response to this anomaly, especially the leading pole of convective heating north of the equator, southwesterlies were thermally induced, leading to further enhanced (suppressed) convection over the SCS–Philippine Sea (EIO). Thus, the anomalous cyclone over the SCS became a dominant system by 20–25 July. As suggested by Wu et al. (2006), such an off-equatorial cyclonic anomaly over the SCS–Philippine Sea should develop further by interacting with the trailing pole of the equatorial dipole heating. On the other hand, the easterly vertical wind shear should also favor the development of off-equatorial convection anomalies in the Northern Hemisphere during the boreal summer (Wang and Xie 1997; Wu et al. 2006). Note that the strong northeasterlies on the northern side of the anomalous cyclone were evidently unfavorable for rainfall over the Yangtze Basin. The thermally forced Rossby wave response to the off-equatorial convective heating (Gill 1980) further suppressed convection over the equatorial zone but extended convection eastward into the western Pacific during 26–31 July, forming a Rossby wave-like coupled circulation–convection system over the SCS–Philippine Sea, as demonstrated by Mao et al. (2010). During the period 1–6 August, convection over the Yangtze Basin became less suppressed as the anomalous coupled circulation–convection system weakened. Subsequently, active convection again took place over the EIO during 7–12 August, while an anomalous anticyclone with strongly suppressed convection developed over the SCS–Philippine Sea, in turn favoring the development of positive rainfall anomalies over the Yangtze Basin.

In short, the entire evolutionary process of this BSISO1 case exhibited features of typical BSISO1 events, and also indicated that the intraseasonal Yangtze rainfall anomalies were not only related to the alternate occurrence of anomalous cyclonic (anticyclonic) circulations over the SCS–Philippine Sea but also to the coupled circulation–convection systems over the South Asian monsoon region.

Figure 3a shows that the BSISO1-related rainfall anomalies explained a large percentage of the variance over the Yangtze Basin. To further show the association between the intraseasonal Yangtze rainfall and the BSISO1 activities, the composite evolution of the BSISO1-related rainfall anomalies during the BSISO1 cycles in summer 1996 is shown in Fig. 6. Significant wet anomalies were indeed observed over the Yangtze Basin during phases 1–3, with the significant anomaly area expanding slightly northeastward, while the opposite situation occurred in phases 5–7, with the Yangtze Basin being dominated by significant dry anomalies. This confirms the existence of a teleconnection between rainfall anomalies over the Yangtze Basin and the anomalous convection over the EIO (as discussed above). In phases 4 and 8, significant anomalies moved to the lower Yellow River, and there were no significant signals over the Yangtze Basin.

Dynamically, the distribution and evolution of rainfall anomalies depend mainly on large-scale circulation anomalies, and so composites of middle-troposphere vertical motion and precipitable water anomalies are presented in Fig. 7. Corresponding to the wet episode over the Yangtze Basin from phase 1 to 3, a slightly northeast-southwest oriented zone with positive precipitable water anomalies was present around north of 25°N, extending from the middle reaches of the Yangtze Basin into the East China Sea. Note the northeastward migration of the center of the maximum anomaly with increasing phase. Negative precipitable water anomalies were confined to the south. In phases 1–3, although significant positive (negative) precipitable water zones were accompanied by ascending (descending) motions, their maximum anomaly centers did not always overlap exactly. In contrast, during the dry phases, negative precipitable water anomalies existed within the latitude band from 25°N to 35°N, although only the anomalies over the lower Yangtze Basin and to its east were statistically significant, while positive precipitable water anomalies prevailed to the south and the north. The centers of great negative water anomaly over the coastal area matched fairly well with those of significant descending anomaly maxima, especially in phases 6 and 7. Obviously, such a flow pattern did not favor Yangtze rainfall.

Based on the atmospheric continuity equation, enhanced ascending (descending) motion in the middle atmosphere depends largely on strong divergence (convergence) in the upper troposphere and/or strong convergence (divergence) in the lower troposphere. Thus, anomalous convergence (divergence) in the lower and upper troposphere might give rise to the anomalous middle-troposphere vertical motion shown in Fig. 7. Figure 8 shows the pressure–latitude cross-section of composite anomalous divergence and divergent winds. During the wet phases over the Yangtze Basin (phases 1–3), a clear meridional–vertical cell was identifiable, with an ascending branch between 25°N and 30°N and a descending branch south of 20°N. Significant low-level convergence and upper-level divergence anomalies were associated with the ascending branch over the Yangtze Basin, while the descending branch resulted from strong low-level divergence and upper-level convergence anomalies. Anomalous southerlies in the lower troposphere transported more moisture into the Yangtze Basin, leading to positive precipitable water anomalies and thus positive rainfall anomalies. The descending motion and related

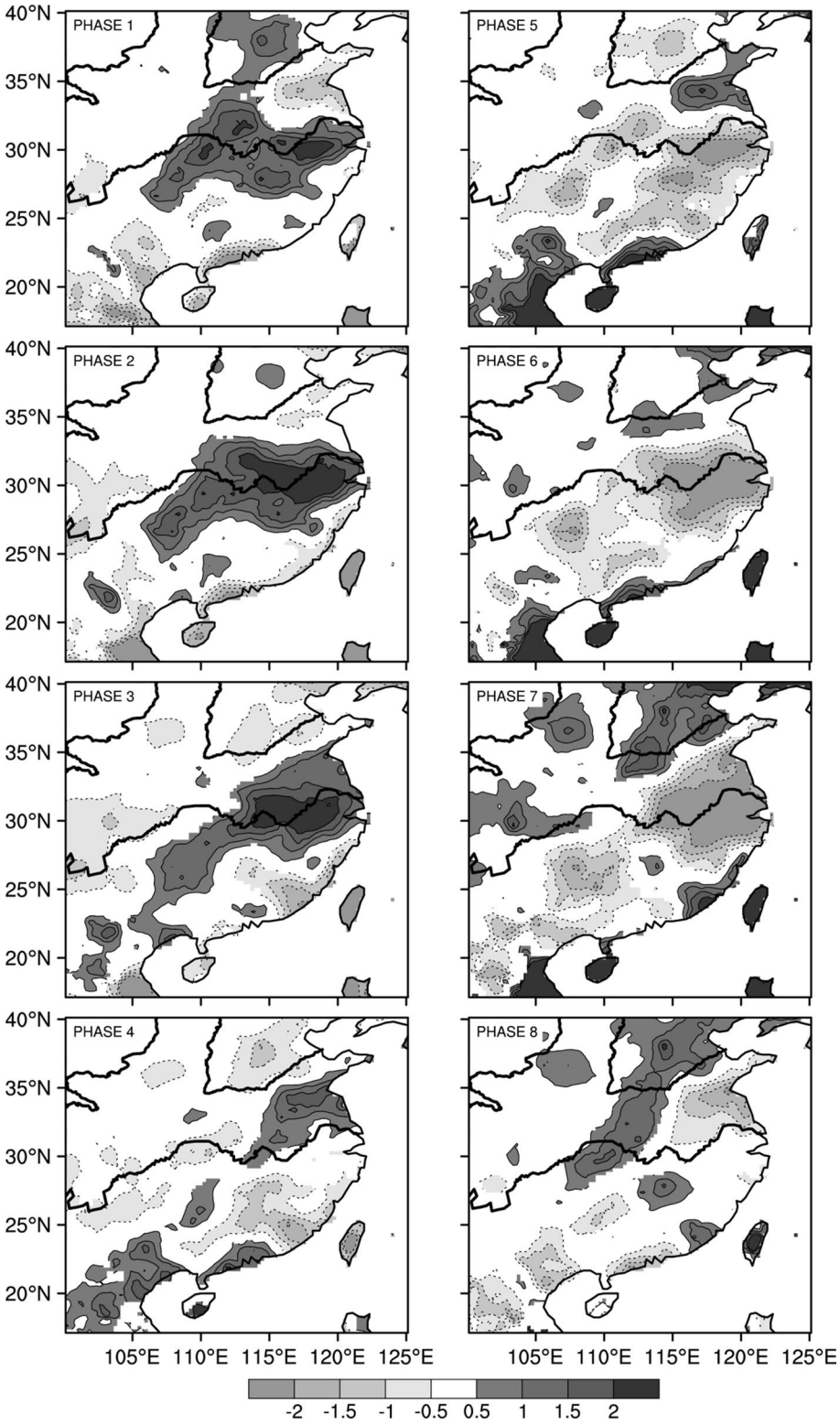

Fig. 6 Evolution of composite BSISO1-related rainfall anomalies (*contours* and *shadings*, mm day^{-1}) over eastern China during a BSISO1 cycle for phases 1–8 in summer 1996 (1 May to 31 October). Only shown are the rainfall anomalies statistically significant at the 95 % confidence level, with *positive* (*negative*) anomalies *shaded darkly* (*lightly*)

mid-tropospheric convergence anomalies in mid-latitudes between 30°N and 40°N might enhance the ascending motion over the Yangtze Basin through a compensation effect. Such implied impacts from mid-latitude systems require further investigation.

By phase 4, the ascending motion over the Yangtze Basin in the middle troposphere became very weak, with the meridional–vertical cell being discernible only in the upper troposphere due to a decrease in both low-level convergence and upper-level divergence. Note that the upper

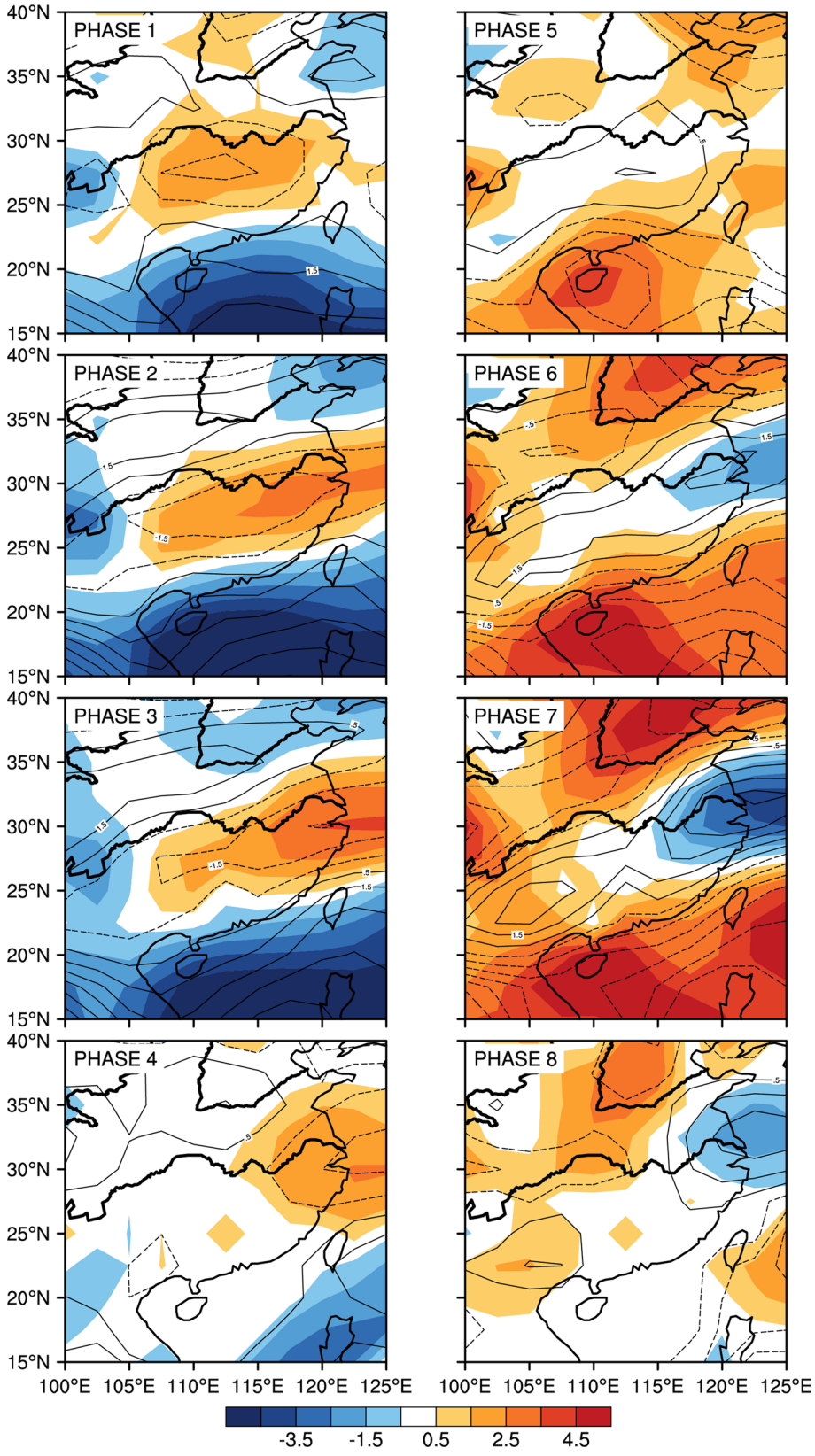

Fig. 7 Evolution of composite anomalous precipitable water integrated from 1000 to 300 hPa (*color scale*, g) and anomalous 500-hPa vertical motion (*contours*, 10^{-2} Pa s^{-1}) during a BSISO1 cycle for phases 1–8 in summer 1996 (1 May to 31 October). The contour interval is 0.5, with the zero contour omitted and negative contours *dashed*. Only shown are the vertical motion anomalies and precipitable water anomalies statistically significant at the 95 % confidence level

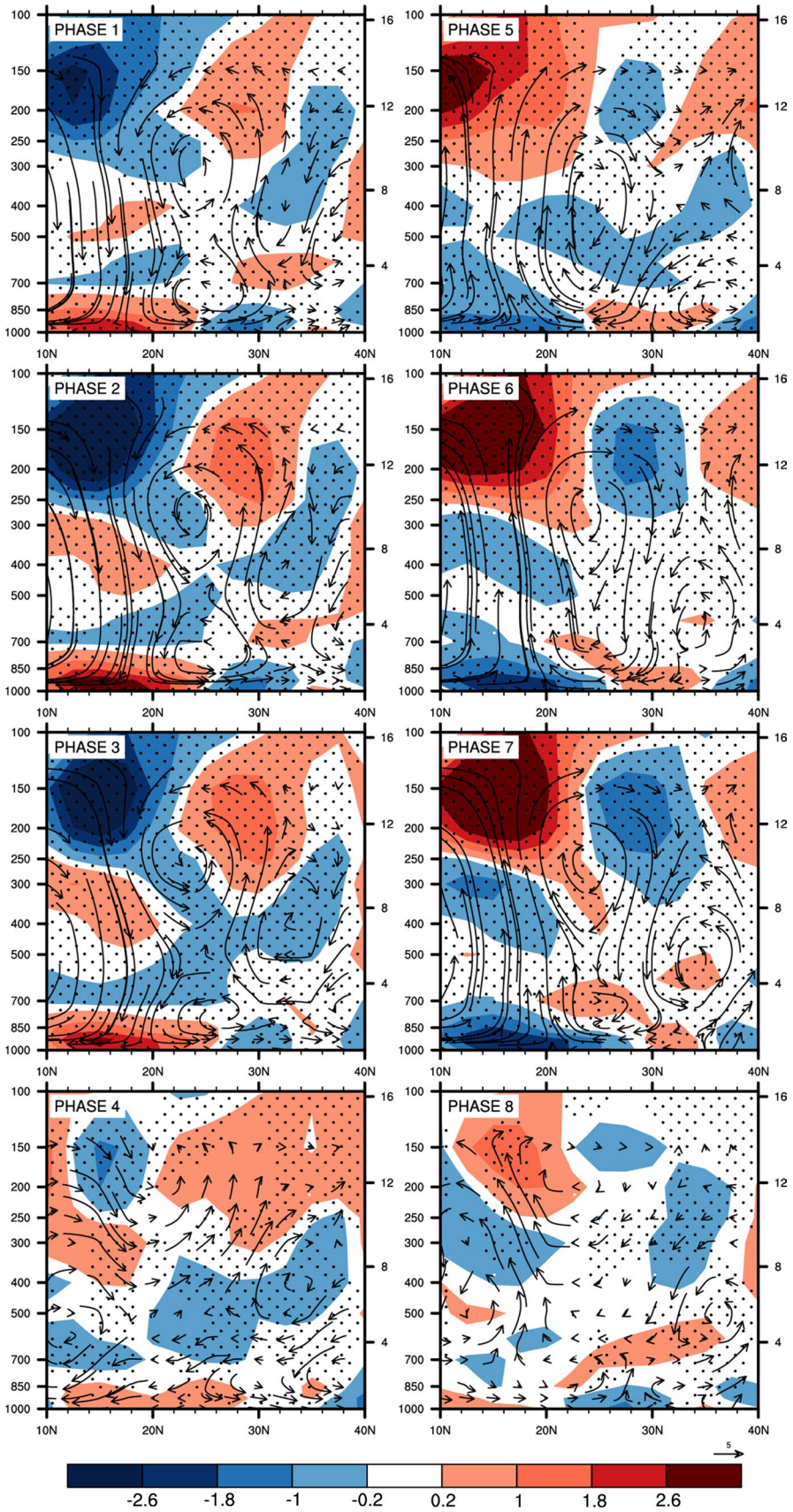

Fig. 8 Pressure–latitude cross-section (110°–120°E) of composite anomalous air flows (*vectors*, meridional divergent wind in m s^{-1}, and omega in 1,000 × Pa s^{-1}) and divergence (*color scale*, 10^{-6} s^{-1}) during a BSISO1 cycle for phases 1–8 in summer 1996 (1 May to 31 October). The *dot-hatching* indicates the regions where the wind and divergence anomalies are both statistically significant at the 95 % confidence level

tropospheric convergence and descending motion over the SCS also weakened. Subsequently, over the SCS, the anomalous convergence in the upper troposphere was replaced by anomalous strong divergence, and anomalous convergence dominated in the lower troposphere in phase 5. The induced strong ascending motion over the SCS, together with the descent to the north, constituted a meridional–vertical cell reversed from phase 1. The descent and low-level northerlies associated with the reversed meridional–vertical cell brought about a dry episode (phases 5–7).

To sum up, the BSISO1 mode initiated over the EIO and propagated eastward as a convectively coupled Kelvin–Rossby wave packet along the equator. After moving over the Maritime Continent, the coupled system veered northward in the form of a Rossby wave-like pattern. The Rossby wave-like coupled convection–circulation system induced an anomalous local meridional–vertical cell over eastern China, with anomalous ascending (descending) motion over the Yangtze Basin and descending (ascending) motion to the south, leading to positive (negative) rainfall anomalies over the Yangtze Basin.

4.2 Impacts of BSISO2

As examined in Sect. 3, the 10–25-day oscillation was another dominant mode modulating the 1996 Yangtze summer rainfall, and such 10–25-day ISOs were closely related to BSISO2 events. One of the two 10–25-day ISOs contributing to the prolonged wet episode of Yangtze rainfall anomalies is selected as an example to show the life cycle of a BSISO2 event in two-dimensional phase space (Fig. 9). This BSISO2 event started on 11 June, indicating that the convective anomaly initially occurred over Southeast Asia (around Southern Borneo). The active convection propagated northwestward, reaching the tropical western Pacific on 17 June, and then stagnated over the SCS–Philippine Sea for around 10 days, finally moved into the East China Sea.

Figure 10 shows the composite evolutions of several BSISO2 events during the 1996 summer in terms of OLR and 850-hPa wind anomalies, to demonstrate how the BSISO2 activities regulate Yangtze rainfall anomalies. Over the EASM region, a weak convective anomaly was first observed around the Maritime Continent (phases 6–7), with a huge anomalous anticyclone to the north. Note that the active convection over the middle Yangtze Basin and southern China in phase 6 arose from anomalous southwesterlies on the northwestern side of the anomalous anticyclone. With northwestward propagation of this anomalous anticyclone, active convection also moved over the middle and lower Yangtze Basin in phases 7 and 8. A distinct anomalous cyclone associated with active convection over the southern SCS can be identified in phase 8. Subsequently, in phase 1, such a convection–circulation system developed further

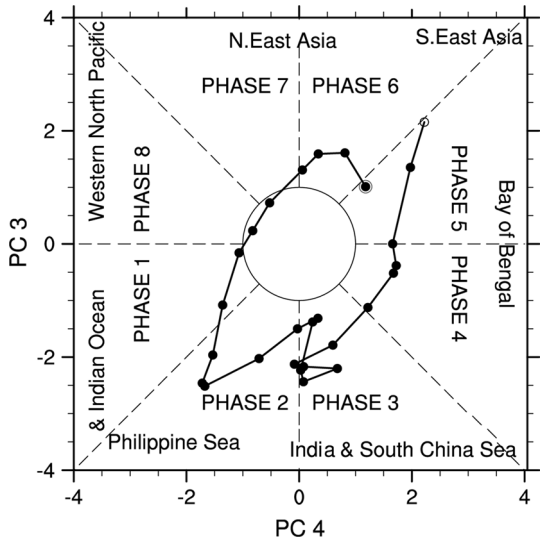

Fig. 9 Phase-space representation of the two-principal-component (PC) BSISO2 index (PC3 and PC4) for the period 11 June to 7 July 1996, with each dot representing the value of the index on a particular day. Also shown are the eight defined phases of the BSISO2 and the region (*central circle*) where the BSISO2 index amplitude $(PC3^2 + PC4^2)^{1/2}$ is <1.0, corresponding to weak activity. The approximate locations of the propagating active convective signal of the BSISO2 are also shown for each quadrant of phase space. *Solid* (*open*) *circle* indicates the *starting* (*end*) point

by interacting with upstream systems over the South Asian sector so that most of the SCS was dominated by active convection, and convection was suppressed over southern China. Note the significantly anomalous cyclonic pair straddling the equator over the EIO. The area of suppressed convection migrated to the middle and lower Yangtze Basin as the cyclonic pair propagated westward from phase 2 to 4. This westward propagation of the anomalous cyclonic pair agrees with that observed by Chen and Chen (1995), who pointed out that the 10–20-day monsoon mode exhibits a double-cell (either double-high or double-low) structure, both of which propagate coherently westward along the equator. The association of the 10–25-day oscillation of the Yangtze rainfall with westward propagation of the equatorial cyclonic pair deserves further research.

The cycle of events described above has many similarities to a typical BSISO2 case (see fig. 10 of Lee et al. 2013). Note that in the evolution of a typical BSISO2 case, focusing on the convective signal over the EASM sector, weak convection actually first occurs over the eastern Maritime Continent in phase 6, strengthens in phase 7, and then propagates northwestward into the SCS–Philippine Sea from phase 8 to 3. In fact, the cyclonic pair structure is also present in phases 2–3, although the southern cyclone is not as distinct as the northern one. This suggests that the 10–25-day oscillation of Yangtze rainfall is indeed dependent on the BSISO2 activities over the entire ASM region.

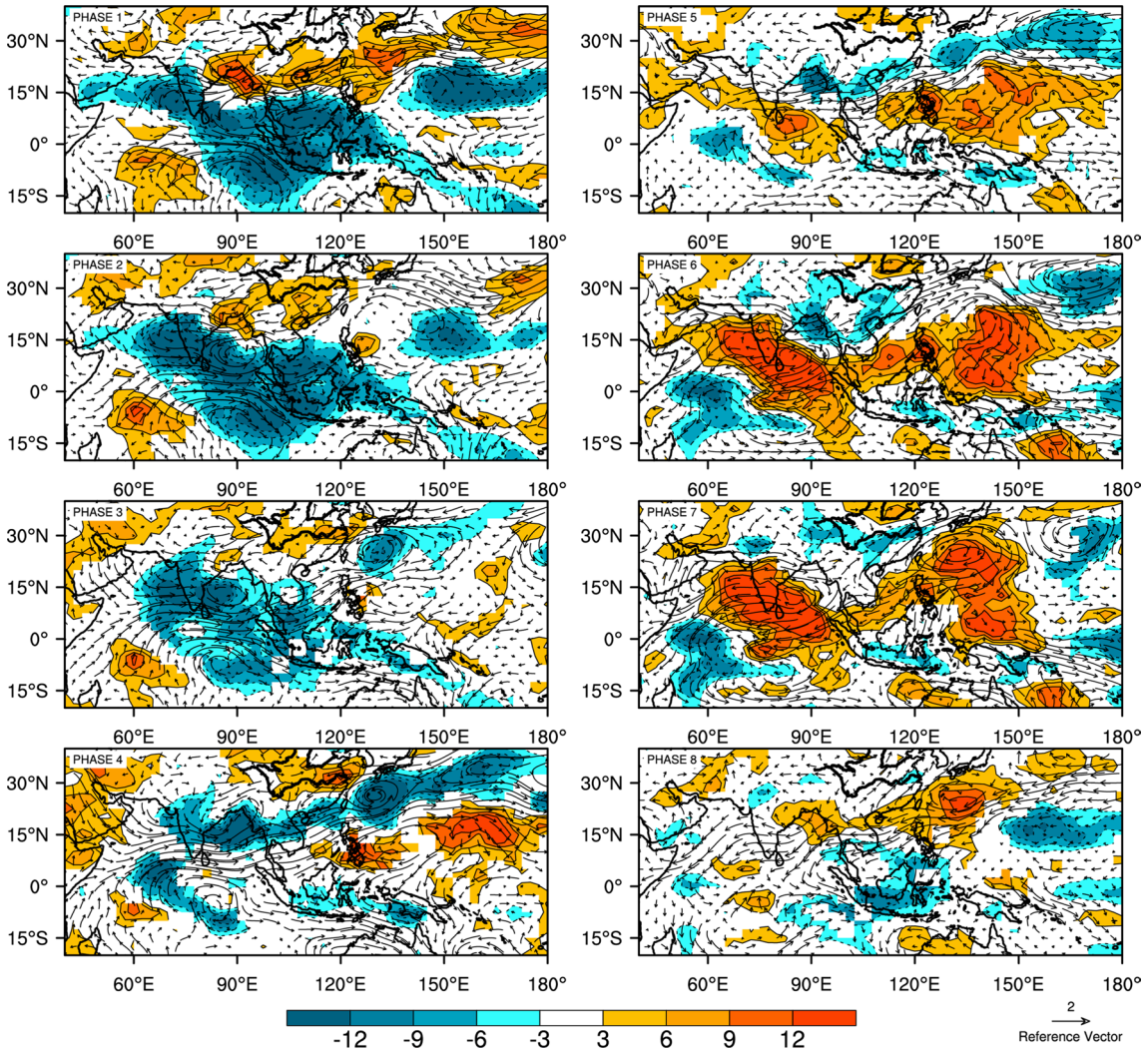

Fig. 10 Evolution of composite OLR (*color scale*, W m^{-2}) and 850-hPa wind (*vectors*, m s^{-1}) anomalies for the BSISO2 cases during the period 1 May–31 October 1996. Only shown are the OLR and wind anomalies statistically significant at the 95 % confidence level. The magnitude of the reference vector is provided at *bottom right*

Note that the convection anomalies over the Philippine Sea were always out of phase with those over the Yangtze Basin, indicating an anomalous local vertical circulation cell. The mid-tropospheric ascents (descents) were often accompanied by upper-level divergence (convergence), and the evolution of the area-averaged divergence at 200-hPa over these two regions is displayed in Fig. 11 to verify the existence of the vertical circulation cell. During phases 2–4, a strong convergence center appeared over the Yangtze Basin, while a divergence center was observed over the Philippine Sea. Again, from the composites of 200- and 925-hPa divergence and divergent wind anomalies during the corresponding phases (not shown), it was found that southeasterlies prevailed from the Philippine Sea to the Yangtze Basin at upper levels, and northwesterlies prevailed from the Yangtze Basin to the Philippine

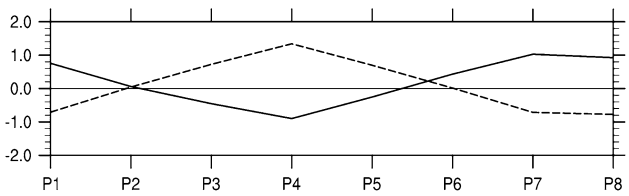

Fig. 11 Composite evolutions of area-averaged 200-hPa divergence anomalies over the Northern Philippine Sea (20°–30°N, 125°–135°E) (*dashed line*, 10^{-6} s^{-1}) and the Yangtze Basin (29°–32°N, 110°–120°E) (*solid line*, 10^{-6} s^{-1}), during a BSISO2 cycle for phases 1–8 in the 1996 summer (1 May–31 October)

Sea at lower levels in phases 2–4. However, in phase 5 the upper-level divergence weakened noticeably. Subsequently, anomalous divergence dominated over the Yangtze Basin,

with strong convergence centered over the Philippine Sea, implying the reversal of the vertical circulation cell.

Consistent with this vertical circulation cell, the BSISO2-related rainfall anomalies demonstrate strong swings over the Yangtze Basin, with positive anomalies occurring in phases 6–8 and negative anomalies in phases 2–4 (Fig. 12). Note that significant rainfall anomalies also appeared over southern China, with patterns reversing between phases 1–4 and phases 5–8. These phase-preference distributions of rainfall anomalies over eastern China can be explained dynamically in terms of vertical motion and precipitable water anomalies (Fig. 13). Anomalous mid-tropospheric ascending motion and enhanced precipitable water were observed across the Yangtze Basin in phases 6–8, leading to enhanced rainfall. In contrast, anomalous descending motion and negative precipitable water anomalies occurred over the lower reaches of the Yangtze Basin during phases 3–4, thus bringing about reduced rainfall over the Yangtze Basin. Again, the evolution of the mid-tropospheric vertical motions verified the existence of the vertical circulation cell. Similarly, rainfall anomaly distributions for each phase over southern China mostly resulted from anomalous vertical motion.

Similar to the impact of BSISO1, the BSISO2 influenced the 10–25-day oscillation of Yangtze rainfall anomalies via anomalous vertical motion and precipitable water, which were in turn modulated by a vertical circulation cell extending from the Philippine Sea to the Yangtze Basin, resulting from the northwestward propagation of BSISO2 activity over the EASM region. The close link between the intraseasonal Yangtze rainfall variations and the westward movement of the equatorial cyclonic pair again indicated that the 10–25-day oscillation of Yangtze rainfall anomalies is related to BSISO2 activity over the entire ASM region.

4.3 Relative importance of the two BSISO modes

Figure 2 suggests that the 1996 Yangtze floods were primarily caused by the anomalous rainfall during major summer months of June–August, which was characterized by unevenly distributed intraseasonal rainfall anomalies, with a distinct prolonged wet episode from late June to mid-July. Further analyses in Sects. 4.1 and 4.2 demonstrate that such intraseasonal Yangtze rainfall anomalies were modulated collaboratively by both BSISO1 and BSISO2 modes. What was the relative role of BSISO1 versus BSISO2 cases in causing the prolonged wet episode? BSISO1 component exhibited strong asymmetry in terms of wet and dry phases (Figs. 4, 6), with the number of days in the wet phases (phases 1–3) exceeding the number of days in the dry phases (phases 5–7). However, the BSISO2 cases did not display such a phase asymmetry (Figs. 9, 12). This indicates that the prolonged wet episode was more influenced by the BSISO1 component.

In fact, the number of the BSISO1-related rainy days (64 days) with positive rainfall anomalies over the Yangtze Basin was indeed much more than that of the BSISO1-related dry days (28 days) during the period June–August (Table 1). In contrast, the BSISO2-related Yangtze rainy days occurred only 33 days, significantly less than the number of dry days (59 days). Such phase-preference statistics again suggest that the seasonal-mean flooding could be attributed mainly to the BSISO1 activity, especially the slower propagation and even stagnation of the strong BSISO1 case (Fig. 4). In turn, the strong BSISO1 case in the 1996 summer in Fig. 5 showed different evolutions during the period from 26 June to 13 July from the typical BSISO1 event (fig. 9 of Lee et al. 2013) during the corresponding period from phase 1 to 3, with strong convection stagnating over the EIO rather than regularly propagating both eastward into the equatorial western Pacific (EWP) and northward into the Indian Subcontinent, implying that during this period the favorable conditions for triggering active convection were not met over the downstream region.

What made active convection stagnant over the EIO for more than 2 weeks? The physical mechanism responsible for the phase stagnation can be understood with reference to the findings of Hsu and Li (2012), who emphasized a key role of the planetary boundary layer (PBL) moisture asymmetry in causing eastward propagation of deep convection, with a positive moisture anomaly ahead of convection center. The positive moisture anomaly in turn sets up a potential unstable stratification. Once the lifting is sufficient enough, potential instability may trigger shallow convection, which further transports moisture upward, leading to the onset of downstream deep convection. Therefore, we examined temporal evolution of the vertical moisture profile over the EWP for this BSISO1 case. The positive moisture anomalies in association with the unstable stratification were observed to occur within the PBL until 11 July 1996 (not shown), indicating that active convection was delayed to develop over the downstream area as compared with the typical BSISO1 event. We further investigated the essential lifting condition for the onset of downstream deep convection. The variation of the anomalous vertical motions in the middle and lower troposphere (weighted average between 1000 and 500 hPa) over the EWP showed that from 26 June to 11 July, strong descending motions prevailed over the EWP, while ascending motions occurred until 12 July, indicating that insufficient lifting was another reason for the phase stagnation. Anomalous vertical motions in the middle-lower troposphere were in turn dependent on the divergent (convergent) conditions of the large-scale circulation in upper/lower troposphere. Such a lower-level convergence center along with the upper-level divergence was actually noted to extend northeastward into the EWP

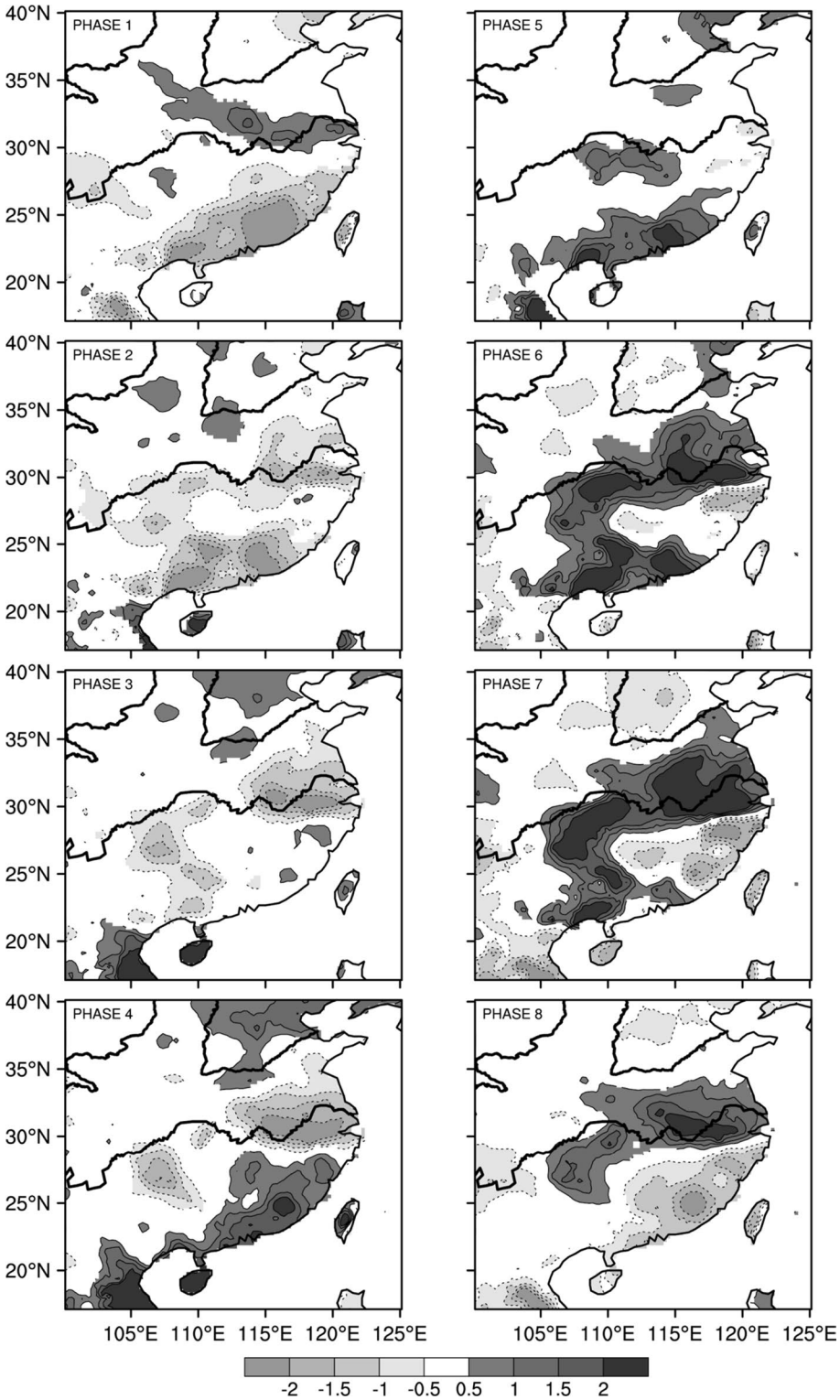

Fig. 12 As in Fig. 6, but for the BSISO2 cases

around 12 July. Active convection was thus initiated due to the release of potential instability.

On the other hand, the IOD may also be one of the external forcings responsible for the wet phase stagnation over the EIO, although Ajayamohan et al. (2008) suggested coherent poleward propagation of precipitation anomalies over the South Asian Monsoon sector during negative IOD years. As a negative IOD year, warm SST anomalies in the southeastern EIO in the 1996 summer were noted to favor stronger convection developing over the EIO and

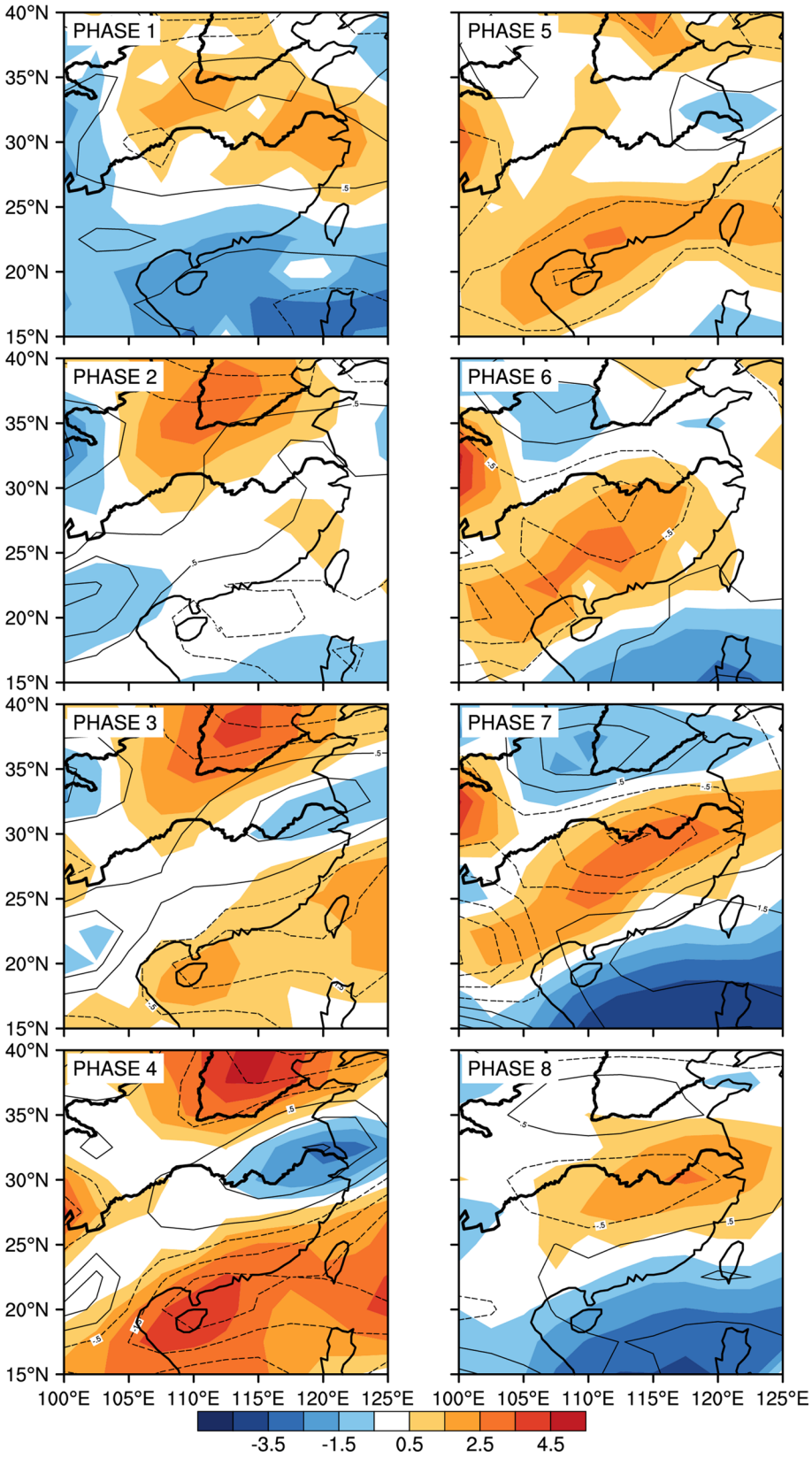

Fig. 13 As in Fig. 7, but for the BSISO2 cases

Table 1 Number of BSISO1-related and BSISO2-related rainy (dry) days when positive (negative) rainfall anomalies occurred over the Yangtze Basin during the period 1 June to 31 August 1996

	Number of rainy days	Number of dry days
BSISO1	64	28
BSISO2	33	59

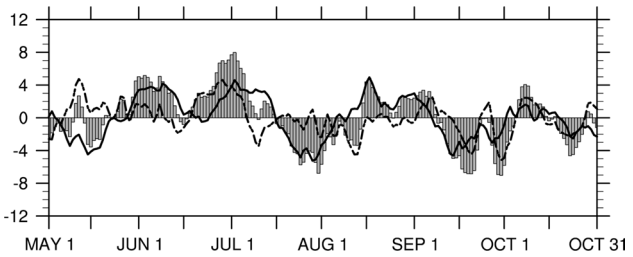

Fig. 14 Time series of the BSISO1-related (*solid line*, mm day^{-1}) and BSISO2-related (*dashed line*, mm day^{-1}) rainfall anomalies, area-averaged over the Yangtze Basin (29°–32°N, 113.5°–122°E) for the period 1 May to 31 October 1996. Also shown is the summation of these two rainfall anomalies (*histogram*, mm day^{-1})

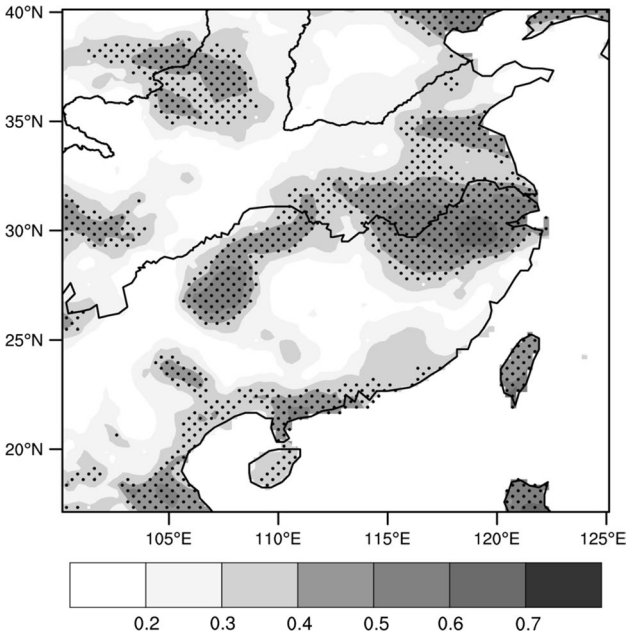

Fig. 15 Correlations (*shading*) between the time series of the actual and BSISO-retrieved rainfall anomalies for the period 1 May–31 October 1996. *Dot-hatching* indicates the regions where the correlation coefficients are statistically significant at the 95 % confidence level

maintaining locally for a longer time (Yuan et al. 2012), thereby decreasing significantly the eastward-propagating speed of active convection. Of course, this issue may involve in air–sea interaction and needs to be further explored in the future.

As seen in Fig. 14, the reduction of area-averaged rainfall over the Yangtze Basin within the prolonged wet episode indeed arose when the BSISO1 wet phases encountered the BSISO2 dry phases, while the overlapping wet phases caused several short-lived extremely heavy rainfall events. Note that although the BSISO1 mode had a much more significant impact than the BSISO2 mode, intraseasonal Yangtze rainfall anomalies were actually the result of the co-modulation of both BSISO modes.

5 Application of BSISO indices to retrieving the intraseasonal Yangtze rainfall

Since each of the two BSISO modes had a statistically significant impact on Yangtze rainfall, and BSISO1- and BSISO2-related rainfall anomalies together accounted for around 40 % of the total intraseasonal variability of Yangtze rainfall during the 1996 summer, we took the 1996 summer as an example to apply the BSISO indices to retrieving intraseasonal Yangtze rainfall. The time series of the BSISO-retrieved rainfall anomalies at each grid point was reconstructed by means of the following procedure. (1) The predominant BSISO mode at a particular time was defined as that with the greater amplitude of the BSISO index, where amplitudes of the BSISO1 and BSISO2 indices were calculated as the root mean square of two PCs as $(PC1^2 + PC2^2)^{1/2}$ and $(PC3^2 + PC4^2)^{1/2}$, respectively. (2) The standardized composite BSISO1 (BSISO2)-related rainfall anomalies were obtained by dividing the BSISO1 (BSISO2)-related rainfall anomalies by the mean amplitude of the BSISO1 (BSISO2) index for each phase of a BSISO1 (BSISO2) cycle. (3) Under the assumption that the intraseasonal rainfall anomalies at a particular time were determined primarily by the predominant BSISO mode, the BSISO-retrieved rainfall anomalies were estimated as the product of the predominant BSISO index and the standardized rainfall anomalies in the corresponding phase of the predominant BSISO mode.

Figure 15 shows the distribution of the correlations between the time series of the actual and BSISO-retrieved rainfall anomalies for the period from 1 May to 31 October 1996. The correlation coefficients over the Yangtze Basin were above 0.6, indicating a feasibility to use BSISO indices as predictors for the intraseasonal rainfall anomalies over the Yangtze Basin. Note that although significant correlations also existed over other regions, only the modulations of the Yangtze rainfall by BSISO modes have been dynamically explained in the present study. Whether the intraseasonal rainfall variability over other regions, such as southern China, could be linked to BSISO modes requires further investigation.

6 Summary and discussion

This research was carried out as a case study considering the fundamental characteristics of the BSISO activity during the 1996 summer and the association of intraseasonal Yangtze rainfall variability with BSISO behaviors over the entire ASM region. The objective was to investigate the physical processes responsible for the ISOs of Yangtze summer rainfall and the potential application of the BSISO indices proposed by Lee et al. (2013) for retrieving the intraseasonal rainfall variability over the Yangtze Basin.

Wavelet analyses suggest that intraseasonal variations of Yangtze rainfall in the 1996 summer were controlled by both 30–60-day and 10–25-day oscillations. The prolonged wet episode from late June to mid-July resulted from a phase-lock between a wet phase of the 30–60-day ISO and two wet phases of the 10–25-day ISO, leading to a seasonal (May–October) rainfall excess above 35 % over the Yangtze Basin, and severe floods. These two dominant ISOs are found to accord well with the BSISO modes in terms of frequency, with BSISO1- and BSISO2-related rainfall anomalies together accounting for around 40 % of the total intraseasonal variability of the Yangtze rainfall, indicating a close association of the intraseasonal variation of Yangtze rainfall with BSISO behaviors over the entire ASM region.

Studies of the circulation show that the entire BSISO1 cycle associated with the prolonged wet episode exhibited similar features to the typical BSISO1 patterns described by Lee et al. (2013). Active convection anomalies were observed to develop first over the EIO with strong convergence of anomalous zonal winds around the equator at the end of June. Westerly anomalies resulted from a cyclone pair on either side of the equator over the Indian Ocean, and easterly anomalies over the Maritime Continent arose from an anomalous anticyclone associated with significantly suppressed convection over the SCS–Philippine Sea. The anomalous southwesterlies on the northwestern side of the anomalous anticyclone converged toward the Yangtze Basin, producing active convection, indicating that intraseasonal convection anomalies over the Yangtze Basin occurred in conjunction with those over the EIO and the SCS–Philippine Sea regions. Over the East Asian sector, a triple convection anomaly pattern extended along the meridian from the Maritime Continent to the Yangtze Basin; this pattern arose from a local meridional–vertical cell associated with the meridional propagation of a Rossby wave-like coupled circulation–convection system. The ascending motion that initiated active convection over the Yangtze Basin was coupled with a descending branch to the south, with the lower tropospheric convergence and upper tropospheric divergence providing the necessary dynamical support. It was indeed the persistence of such a flow pattern that brought about the prolonged wet episode. The percentage of wet phases was higher in BSISO1 cases than in BSISO2 cases, implying that the Yangtze flood in the 1996 summer was primarily due to slower propagation and even stagnation of the BSISO1 component.

Unlike the BSISO1 case, in the BSISO2 case the weak convective anomaly was first initiated over the EASM region around the Maritime Continent, with a huge anomalous anticyclone accompanied by suppressed convection over the SCS–Philippine Sea. Southwesterly anomalies were associated with the anomalous anticyclone, forming low-level convergence and consequent strong ascending motion over the Yangtze Basin, leading to positive rainfall anomalies. Subsequently, the anomalous anticyclone migrated northwestward and weakened, with the active convection over the Yangtze Basin moving slightly northeastward. Meanwhile, the weak convective anomaly became active with a distinct anomalous cyclone appearing over the SCS. This coupled system further developed by interacting with upstream systems over the South Asian sector and dominated the entire SCS and tropical Indian Ocean, while convection was suppressed over the Yangtze Basin. The entire cycle of the BSISO2 mode resembled the typical BSISO2 events described in Lee et al. (2013), suggesting that the 10–25-day oscillation of Yangtze rainfall was indeed dependent on BSISO2 activity over the entire ASM region during summer 1996.

Based on the statistically significant impacts of the BSISO modes on Yangtze rainfall, BSISO indices have been used to retrieve the intraseasonal rainfall anomalies. The correlation coefficients between the time series of the actual and BSISO-retrieved rainfall anomalies over the Yangtze Basin exceeded 0.6, implying the potential application of BSISO indices to retrieving the intraseasonal Yangtze rainfall.

It should be noted that although this case study demonstrates well the association of the ISOs of Yangtze rainfall with both BSISO1 and BSISO2 events over the entire ASM region, this situation may not be the norm for all other summers. For example, as shown by Mao et al. (2010), the dominant ISO period of the Yangtze rainfall during the 1993 summer was 10–20 days, which implies that the intraseasonal Yangtze rainfall could be influenced only by BSISO2 events. Moreover, this case study seems to show the Yangtze flooding being related to the BSISO events, but such a situation may not always hold in other years. Indeed, the dominant ISO period of the Yangtze rainfall during the 1982 summer was found to be 20–50 days (Mao et al. 2010), but no flooding took place that year. In addition, it is unclear how the ISOs of the Yangtze rainfall are related to the BSISO events during a positive IOD year. Nevertheless, the present results can provide a basic scenario for further investigation into other possible impacts or links, such as how and to what extent mid-latitude systems modulate the

intraseasonal Yangtze rainfall. Of course, the convective origin of the BSISO2 event and its propagation in relation to the 10–25-day oscillation of the Yangtze rainfall need to be further examined in more case studies, with numerical experiments to validate the driving mechanisms.

Acknowledgments NCEP/NCAR reanalysis data were obtained from the NOAA–CIRES Climate Diagnostics Center, Boulder, Colorado. This research was jointly supported by the National Basic Research Program of China (2014CB953902, 2011CB403505, and 2012CB417203), the Priority Research Program of the Chinese Academy of Sciences (XDA01020302), and the Natural Science Foundation of China (41175059 and 41375087).

References

Ajayamohan RS, Rao SA, Yamagata T (2008) Influence of Indian Ocean dipole on poleward propagation of boreal summer intraseasonal oscillations. J Clim 21:5437–5454

Bhat GS (2006) The Indian drought of 2002: a sub-seasonal phenomenon. Q J R Meteorol Soc 132:2583–2602

Bretherton CS, Widmann M, Dymnikov VP, Wallace JM, Blade I (1999) The effective number of spatial degrees of freedom of a time-varying field. J Clim 12:1990–2009

Chen TC, Chen JM (1995) An observational study of the South China Sea monsoon during the 1979 summer: onset and life cycle. Mon Weather Rev 123:2295–2318

Chen TC, Yen MC, Weng SP (2000) Interaction between the summer monsoon in East Asia and the South China Sea: intraseasonal monsoon modes. J Atmos Sci 57:1373–1392

Gill AE (1980) Some simple solutions for heat-induced tropical circulation. Q J R Meteorol Soc 106:447–462

Guan B, Chan JCL (2006) Nonstationarity of the intraseasonal oscillations associated with the western North Pacific summer monsoon. J Clim 19:622–629

Hoyos CD, Webster PJ (2007) The role of intraseasonal variability in the nature of Asian monsoon precipitation. J Clim 20:4402–4424

Hsu PC, Li T (2012) Role of the boundary layer moisture asymmetry in causing the eastward propagation of the Madden–Julian oscillation. J Clim 25:4914–4931

Huang F, Huang S, Zhang X (2008) Study on the climatological intraseasonal oscillation of Chinese rainfall. Period Ocean Univ China 38(2):173–177

Huang MP, Lin JL, Wang W, Kim D, Shinoda T, Weaver SJ (2013) MJO and convectively coupled equatorial waves simulated by CMIP5 climate models. J Clim 26:6185–6214

Jones C, Carvalho LMV, Higgins RW, Waliser DE, Schemm JKE (2004) Climatology of tropical intraseasonal convective anomalies: 1979–2002. J Clim 17:523–539

Kanamitsu M et al (2002) NCEP dynamical seasonal forecast system 2000. Bull Am Meteorol Soc 83:1019–1037

Krishnamurti TN, Subrahmanyam D (1982) The 30–50 day mode at 850 mb during MONEX. J Atmos Sci 39:2088–2095

Lau KM, Chan PH (1986) Aspects of the 40–50 day oscillation during the northern summer as inferred from outgoing longwave radiation. Mon Weather Rev 114:1354–1367

Lau KM, Peng L (1987) Origin of low-frequency (intraseasonal) oscillations in the tropical atmosphere. Part I: basic theory. J Atmos Sci 44:950–972

Lau KM, Yang GJ, Shen SH (1988) Seasonal and intraseasonal climatology of summer monsoon rainfall over East Asia. Mon Weather Rev 116:18–37

Lawrence DM, Webster PJ (2001) Interannual variations of the intraseasonal oscillation in the South Asian summer monsoon region. J Clim 14:2910–2922

Lawrence DM, Webster PJ (2002) The boreal summer intraseasonal oscillation: relationship between northward and eastward movement of convection. J Atmos Sci 59:1593–1606

Lee JY, Wang B, Wheeler MC, Fu XH, Waliser DE, Kang IS (2013) Real-time multivariate indices for the boreal summer intraseasonal oscillation over the Asian summer monsoon region. Clim Dyn 40:493–509

Liebmann B, Smith CA (1996) Description of a complete (interpolated) outgoing longwave radiation dataset. Bull Am Meteorol Soc 77:1275–1277

Madden RA, Julian PR (1971) Detection of a 40–50 day oscillation in the zonal wind in the tropical Pacific. J Atmos Sci 28:702–708

Madden RA, Julian PR (1972) Description of global-scale circulation cells in the Tropics with a 40–50 day period. J Atmos Sci 29:1109–1123

Mao J, Chan JCL (2005) Intraseasonal variability of the South China Sea summer monsoon. J Clim 18:2388–2402

Mao J, Wu G (2006) Intraseasonal variations of the Yangtze rainfall and its related atmospheric circulation features during the 1991 summer. Clim Dyn 27:815–830

Mao J, Sun Z, Wu G (2010) 20–50-day oscillation of summer Yangtze rainfall in response to intraseasonal variations in the subtropical high over the western North Pacific and South China Sea. Clim Dyn 34:747–761

Murakami T, Nakazawa T (1984) On the 40–50 day oscillation during the 1979 Northern Hemisphere summer. Part I. Phase propagation. J Meteorol Soc Jpn 62:440–468

Saji NH, Goswami BN, Vinayachandran PN, Yamagata T (1999) A dipole mode in the tropical Indian Ocean. Nature 401:360–363

Torrence C, Compo GP (1998) A practical guide to wavelet analysis. Bull Am Meteorol Soc 79:61–78

Waliser DE, Lau KM, Stern W, Jones C (2003) Potential predictability of the Madden–Julian oscillation. Bull Am Meteorol Soc 84:33–50

Wang B, Rui H (1990) Dynamics of the coupled moist Kelvin–Rossby wave on an equatorial β-plane. J Atmos Sci 47:397–413

Wang B, Xie X (1997) A model for the boreal summer intraseasonal oscillation. J Atmos Sci 54:72–86

Webster PJ, Magana VO, Palmer TN, Shukla J, Tomas RA, Yanai M, Yasunari T (1998) Monsoons: processes, predictability, and the prospects for prediction. J Geophys Res 103(C7):14451–14510

Wheeler MC, Hendon HH (2004) An all-season real-time multivariate MJO index: development of an index for monitoring and prediction. Mon Weather Rev 132:1917–1932

Wheeler MC, Hendon HH, Cleland S, Meinke H, Donald A (2009) Impact of the Madden–Julian oscillation on Australian rainfall and circulation. J Clim 22:1482–1498

Wu MLC, Schubert SD, Suarez MJ, Pegion PJ, Waliser DE (2006) Seasonality and meridional propagation of the MJO. J Clim 19:1901–1921

Yang J, Wang B, Wang B, Bao Q (2009) Biweekly and 21–30-day variations of the subtropical summer monsoon rainfall over the lower reach of the Yangtze River Basin. J Clim 23:1146–1159

Yatagai A, Arakawa O, Kamiguchi K, Kawamoto H, Nodzu MI, Hamada A (2009) A 44-year daily gridded precipitation dataset for Asia based on a dense network of rain gauges. Sola 5:137–140

Yatagai A, Kamiguchi K, Arakawa O, Hamada A, Yasutomi N, Kitoh A (2012) APHRODITE constructing a long-term daily gridded precipitation dataset for Asia based on a dense network of rain gauges. Bull Am Meteorol Soc 93:1401–1415

Yuan Y, Yang H, Li C (2012) Possible influences of the tropical Indian Ocean dipole on the eastward propagation of MJO. J Trop Meteor 28:735–742 (in Chinese)

Zhang C (2005) Madden–Julian oscillation. Rev Geophys 43:RG2003. doi:10.1029/2004RG000158

Zhou W, Chan JCL (2005) Intraseasonal oscillations and the South China Sea summer monsoon onset. Int J Climatol 25:1585–1609

Zhu C, Nakazawa T, Li J, Chen L (2003) The 30–60 day intraseasonal oscillation over the western North Pacific Ocean and its impacts on summer flooding in China during 1998. Geophys Res Lett 30(18):1952. doi:10.1029/2003GL017817